Moist moss tundra on Kapp Linne, Svalbard is a net source of CO_2 and CH_4 to the atmosphere

A. Lindroth[1], N. Pirk[2], I. S. Jónsdóttir[3], C. Stiegler[4], L. Klementsson[5], and M. B. Nilsson[6]

[1]Department of Physical Geography and Ecosystem Science, Lund University, Lund, Sweden.

[2]Department of Geosciences, University of Oslo, Oslo, Norway.

[3]Life and Environmental Sciences, University of Iceland, Reykjavik, Iceland.

[4]Bioclimatology, Georg-August Universität Göttingen, Göttingen, Germany.

[5]Department of Earth Sciences, University of Gothenburg, Gothenburg, Sweden.

[6]Department of Forest Ecology and Management, Swedish University of Agricultural Sciences, Umeå, Sweden.

Corresponding author: anders.lindroth@nateko.lu.se

Key Points:

- A moist moss tundra in Svalbard is a small net source of CO_2 and CH_4 on an annual basis
- Temperature sensitivity during summer is higher for gross primary productivity than for ecosystem respiration at low temperature (0-4.5 ºC) and the opposite at higher temperature
- A modest temperature increase of 1 degree increases ecosystem respiration and gross primary productivity of similar magnitude during summer but strengthens the annual source of CO_2
- Greenness index contribute significantly to explain variation in both carbon dioxide and methane fluxes

Abstract

We used dark chamber measurements for CO_2 and CH_4 fluxes and eddy covariance for CO_2 fluxes to quantify the fluxes and to study their environmental controls from a moist moss tundra in Svalbard. The net ecosystem exchange (NEE) during the summer (June-August) was on average -0.40 g C m^{-2} day^{-1}or -37 g C m^{-2} for the whole summer. Including also the spring and autumn periods the NEE was reduced to -6.8 g C m^{-2} and the annual NEE became positive, 15.2 gC m^{-2} due to the losses during the winter. The CH_4 flux which was only measured during the summer period showed a large spatial and temporal variability. The mean value of all 214 samples was 0.000511±0.000315 µmol $m^{-2}s^{-1}$ which corresponds to a growing season estimate of 0.04 to 0.16 g CH_4 m^{-2}. Converting these emissions to CO_2-equivalents using a global warming potential of 34 we find that this moss tundra emits about 60 gCO_2-equivalents m^{-2} yr^{-1} of which CH_4 is responsible for 7%.

Air temperature, soil moisture and greenness index contributed significantly to explain the variation in ecosystem respiration (R_{eco}) while active layer depth, soil moisture and greenness index were the variables that best explained CH_4 emissions. Estimate of temperature sensitivity of R_{eco} and gross primary productivity showed that a modest increase in air temperature of 1 degree did not significantly change the NEE during the growing season but that the annual NEE would be even more positive adding another 8.5 gC m^{-2} to the atmosphere. We tentatively suggest that the warming of the Arctic that has already taken place is partly responsible for the fact that the moist moss tundra now is a source of CO_2 to the atmosphere.

1 Introduction

Climate warming is predicted to be most evident at high latitudes (Friedlingstein et al., 2006) with profound effects on ecosystem functioning. One of the high latitude regions that are expected to experience the most dramatic changes caused by climate change is the Arctic. This region which is located roughly north of the tree-line is characterized by cold winters and cool summers and with mean annual temperatures below zero. The summer periods are short ranging between 3.5 to 1.5 months from the southern boundary to the north and July is normally the warmest month. Annual precipitation is generally low decreasing from about 250 mm in the southern areas to 45 mm in polar deserts in the north (Callaghan et al., 2005).

The permafrost soils in the Arctic store 1035±150 Pg of organic carbon in the top 0-3 m (Hugelius et al., 2014) which is more than the average 2010-2019 of 860 Pg of carbon in the atmosphere (Friedlingstein et al., 2020). The increased warming in these areas can induce higher decomposition rates due to increased microbial activity which will provide a positive feedback to the climate system (Schuur et al., 2015). On the other hand, warming can also increase photosynthesis and carbon uptake and thus compensate for, or exceed, the effect of increased decomposition. Climate warming is also affecting plant community composition and the length of the growing season (Post et al., 2009) which also has an impact on the processes regulating annual carbon emissions and uptake (Bosiö et al., 2014). There is however a large uncertainty regarding the timing, magnitude and possible sign of potential feedbacks caused by these changes (Myers-Smith et al., 2020).

Understanding processes that are controlling the exchanges of greenhouse gases in the Arctic is crucial for assessment of potential feedback effects. For this purpose, multiple year-around long-

term studies including direct measurements of CO_2 and CH_4 fluxes covering all seasons, winter, spring, summer and autumn would be ideal. This is a great challenge in the harsh climate of the Arctic and with limited support of key infrastructures for, e.g., provision of electricity for operation of instruments.

In spite of these difficulties a few year-around studies have been performed during the last couple of decades. In the low Arctic, Oechel et al. (2013) demonstrate the importance of the wintertime fluxes in a tussock tundra ecosystem in Alaska. They found that the non-summer season emitted more CO_2 than the corresponding uptake during the summer resulting in a net source to the atmosphere of about 14 gC m^{-2} on an annual basis. They also showed that the shoulder seasons, spring and autumn roughly out-weighted the summer uptake. Euskirchen et al. (2012, 2016) measured net CO_2 exchange in three different tundra ecosystems; heath tundra, tussock tundra and wet sedge tundra in northern Alaska over three years. They found that the uptake of -51 to -95 gC m^{-2} during the summer (June-August) was overturned by the respiration that occurred during the winter period resulting in net annual losses for all three ecosystems. Zhang et al. (2019) reported five years of year-around flux measurements in a heath ecosystem on west Greenland and they found that the heath was an annual sink of -35±15 gC m^{-2}. One year with an anomalously deep snow pack showed a 3-fold higher respiration during the winter as compared to the other years which resulted in a significantly lower net uptake during that year.

Even fewer studies have been done on year-roud studies in the high Arctic. Lüers et al. (2014) quantified the annual CO_2 budget using eddy covariance measurements in a river catchment area near Ny-Ålesund on Spitsbergen in the Svalbard archipelago and they found that the ecosystem was in C-balance. The footprint area was a semi-polar desert with only 60% vegetation cover and patches of bare soil and stones. Also in Svalbard but further south in Adventdalen on a flat alluvial fen irregularly covered with ice wedged polygons, Pirk et al. (2017) made year-around measurements of CO_2 fluxes and found it to be a net sink of -82 gC m^{-2}. Because of the irregularities caused by the ice wedges and the differences in wetness, they focused the analyses on the spatial variability in two different directions, one wetter and one drier, and they estimated the annual net ecosystem exchange to -91 gC m^{-2} and -62 gC m^{-2} for the respective areas.

The Arctic ecosystems constitute also a source of CH_4 to the atmosphere even if it is not a very large one. Saunois et al. (2020) estimated that the Northern high latitude region (60ºN - 90ºN) contributed 4% of global emissions and emissions from wetlands are only part of the emissions from this region. However, in the light of the vulnerability of the high Arctic permafrost areas and considering the large carbon pool and the predicted changes in climate, a quantification and understanding of CH_4 exchanges in these areas are still important. Christensen et al. (2004) showed one example of a dramatic impact of the climate warming on the CH_4 emissions in a permafrost mire in sub-arctic Sweden. The warming which is visible in this area since decades and its impact on permafrost and vegetation changes was estimated to have caused an increase of landscape CH_4 emissions in the range 22-66% in the period 1970 to 2000.

Mastepanov et al. (2008) were the first to show the importance of emissions also outside of the growing season. They observed a large burst of CH_4 from a fen area in Zackenberg, Greenland after the growing season and during the time when the soil started to freeze. This finding was confirmed in a later paper (Mastepanov et al., 2013) and the process was hypothetically

attributed to the subsurface CH_4 pool. Hydrology and vegetation composition play an important role for CH_4 emission and dynamics. McGuire et al. (2012) made a comprehensive summary of CH_4 exchanges of the Arctic tundra showing the difference between wet and dry ecosystems; the wet tundra emitted 5.4 to 13.0 gCH_4-C m^{-2} during summer and 8.5 to 20.2 gCH_4-C m^{-2} annually. The corresponding values for the dry/mesic tundra were 0.3 to 1.4 gCH_4-C m^{-2} and 0.3 to 4.3 gCH_4-C m^{-2}, respectively. Bao et al. (2021) utilized year-around measurements of CH_4 fluxes from three sites of the Ameriflux network in Northern Alaska to demonstrate the importance of the spring and autumn seasons for the annual emission. The shoulder seasons contributed about 25% of the annual emissions and the autumn season had about three times higher emission than the spring season. These findings increasingly emphasise the importance of year-around measurements to fully understand the CH_4 controls and dynamics.

The main aim of this study is to provide another piece of the puzzle concerning CO_2 and CH_4 exchanges from different but widespread ecosystem types in the high Arctic. We hypothesise that this moist tundra ecosystem is a net annual carbon sink and that the summer emissions of methane will be at average levels. We made flux measurements of CO_2 and CH_4 in an moist moss tundra ecosystem situated at Kapp Linne on the west coast of the Svalbard archipelago in 2015 and with an additional campaign in 2016. The measurements in 2015 were done using both eddy covariance system (CO_2) and chambers (CO_2 and CH_4) but only chambers in 2016. We quantify ecosystem respiration (R_{eco}), gross primary productivity (GPP) and net ecosystem exchange (NEE) during the growing season based on measurements and we extend the time period to a full year by modelling. The CH_4 emission was only quantified for the summer season. We also analyze the environmental controls of the fluxes.

2 Materials and Methods

2.1 Research site and measurements

This study was performed in the Svalbard archipelago near the weather station Isfjord Radio (78°03′08″N 13°36′04″E, alt. 7 m) which is located right on the foreland of Kapp Linné on the island of Spitzbergen (Fig. S1). The tundra area where the measurements were performed is located about 1 km southeast of the station. The study area consists of moist moss tundra, a widespread ecosysetem in Svalbard (Vanderpuye et al., 2002; Ravolainin et al., 2020). The vegetation is characterised by the moss species *Tomentypnum nitens, Sanionia uncinata* and *Aulocomium palustre* and a sparse cover of vascular plants (20-40%), dominated by *Equisetum arvense*, *Salix polaris* and *Bistorta vivipara*. Other vascular plant species found in the plots: *Saxifraga cespitosa*, *Saxifraga oppositifolia*, *Silene aucaulis*, and some grass species, most likely *Alopecurus ovatus* (previously *A. borealis*), and *Poa arctica*. The vegetation analysis was made from photographs of chamber location plots taken between 26 June and 2 July 2015 (see Figs. S4a-4y in Supplement).

The net ecosystem exchange of CO_2 was measured with an eddy covariance (EC) system located centrally on the moss tundra (78°03′28.6″N 13°38′40″E). The sonic anemometer (USA-1; Metek GmBH, Germany) was mounted on top of a tripod (see Fig. S1) at 2.7 m height. The CO_2 and H_2O concentrations were measured with an open path sensor (LI-7500; Li-Cor Inc., USA) placed just beneath the sonic and inclined about 30º pointing towards east. Radiation components,

incoming and outgoing short-wave and long-wave (CNR-4; Kipp & Zonen, the Netherlands) were measured at 2.0 m height above ground with the sensor directed towards south. All sensors were connected to a datalogger (CR-1000; Campbell Scientific, USA) which was powered by a solar panel and a battery. The EC sensors were sampled and stored at 10Hz and all oter sensors were sampled at 0.1Hz with storage of 30 min mean values. These measurements were made from 25 June to 17 September 2015.

The soil efflux of CO_2 and CH_4 was measured with a dark chamber connected to a gas analyzer (Ultraportable Greenhouse Gas Analyzer; Los Gatos Research, USA) on 24 locations within the EC average footprint area. A circular thin-steel frame, 15 cm in diameter and 15 cm high, was inserted ca 5 cm into the ground in each location. The sharp edge of the frames made it easy to insert them into the ground without damaging the vegetation and with minimal soil disturbance. A picture was taken of each frame (see Supplement) for documentation of vegetation and for calculation of different indexes. The chamber was also made from steel and it had a rubber seal in the end facing the frame (Fig. S2) to make it air tight when mounted on the frame. The volume of the chamber and the part of the frame raised above the surface was 5.3 L. A small fan was installed inside the chamber to provide good mixing of the air during measurement. A small weight (stone) was placed on top of the chamber during measurement to prevent it from moving due to wind gusts. During concentration measurement air was circulated in a closed loop between the chamber and the gas analyzer in ca. 10 m long 4 mm diameter polyethene tubes (see Fig. S2). The air flow through the analyzer was ca 1.2 L min^{-1}. The chamber was ventilated in the free air about 1 minute before each measurement which lasted for 5 minutes. The concentrations were recorded and stored once per second by the gas analyzer. The time stamp of the recorded data was used to identify measurement cycles for analysis of fluxes.

The chamber measurement positions were selected in the following way. The frames were grouped in two sections, one north-east and one south-west of the flux tower since it was expected that the main wind direction would be along that direction. Each group was then split into three subsections with four measurement points within each one of them. The locations were named S1:1-S1:4, S2:1-S2:4, S3:1-S3:4, N1:1-N1:4, N2:1-N2:4 and N3:1-SN3:4. The four measurement points within each subsection were then placed along a transect with 3-4 m between each point. This way it was possible to measure all four chamber locations without having to move the whole measurement system. Chamber measurements were made in three separate campaigns: mid-summer (26 June to 2 July 2015), late-summer (25-27 August 2015) and early-summer (14-15 June 2016). Each location was measured three times during each one of the three campaigns, a total of 216 measurements. Besides gas concentrations, also soil temperature (5 cm), soil moisture (0-5 cm) and active layer depth was measured during each campaign.

Meteorological data needed for analyses and gap-filling were obtained as follows: Hourly air temperature and relative humidity from Isfjord radio, half-hourly global radiation from Adventdalen, daily snow depth and ground ice conditions from Svalbard airport and monthly precipitation from Isfjord radio and Barentsburg. The distance between the measurement site and these stations are; Isfjord radio, 1 km, Barentsburg, 13 km, Svalbard airport, 46 km and Adventdalen, 50 km. Data sources are given in Acknowledgement.

3. Data analysis

The rawdata from the eddy covariance flux measurements were analysed using the Eddypro software version 6.1.0 (Li-Cor, 2016). Correction was made for the impact of the additional heat flux in the sensor path of the open path analyzer on the flux calculations according Burba et al. (2008). Gap filling during the measurement period was made using the REddyProc online eddy covariance data processing tool developed at the Max Planck Institute for Biogeochemistry (Wutzler et al., 2018) without u* correction since we could not identify any specific u* threshold. Only data of highest quality, i.e. class=0 was retained for the gap filling and further analyses. Gap filling outside of the EC measurement period to obtain the carbon balance for a full year was made using empirical relationships for R_{eco} and GPP (see below).

For flux footprint calculations the roughness length (z_0) is needed and it was calculated from the wind profile relationship in near neutral (-0.01<z/L<0.01) conditions:

$$z_0 = \frac{z_m}{e^{(u(z)\cdot\frac{k}{u^*})}} \quad (1)$$

where z_m is measurement height, u(z) is wind speed at height z, k is von Karman's constant and u* is friction velocity. We used the flux footprint prediction (FFP) online tool by Kjun et al. (2015) to calculate the footprint climatology.

The fluxes from the chamber measurements were estimated from the time change of the concentrations using linear regression. Every individual measurement was inspected and evaluated manually. These inspections showed that 50 seconds for CO_2 and 100 seconds for CH_4 were optimal to obtain near perfectly linear responses a few seconds after the chamber had been placed on the frame. The slopes of the regressions were then used to calculate fluxes per unit surface area. The flux detection limits for CO_2 and CH_4 were calculated in the following way: first the peak-to peak variation in the respective gases were determined when the chamber was ventilated in the free air and when conditions were steady. Then 20 sets of artificial 'fluxes' for each gas species were estimated based on 100 randomly generated concentrations for each data set. The peak-to-peak difference was used as seed (input) for the randomly generated values. The 95% value of the distribution of these randomly generated fluxes was taken as the flux detection limit for the respective gas.

The pictures of the vegetation inside of the chamber frames were analysed using the ImageJ (https://imagej.net) public domain software. The camera color channel information (digital numbers for Red (R), Green (G) and Blue (B) channels) was collected from the JPEG pictures. This type of pictures is for instance used in studies that are tracking the phenological development of vegetation (e.g. Richardson et al., 2009). The so-called green index (GI) is applied to detect differences in greenness of vegetation:

$$GI = G/(R+G+B) \quad (2)$$

This index was also estimated for the central footprint area (100 m radius) of the flux measurement location using a picture taken at 160 m above the altitude of the measurement area.

Forward stepwise linear regression (Sigmaplot 12.5) was used to analyze the dependency of the CO_2 and CH_4 fluxes on environmental variables. We tested for air temperature (T_a), soil moisture (θ), soil temperature (T_s), active layer depth (ALD), measurement location (S_{id}) and GI.

For gap filling of R_{eco} we only had access to air temperature with full annual coverage and, thus, we could only use this driver for estimation of the R_{eco}. The measured chamber CO_2 fluxes were fitted to the Lloyd & Taylor (1994) model with air temperature (T_a) as independent variable:

$$FCO_2 = a \cdot e^{b\left(\frac{1}{56.02} - \frac{1}{T_a + 46.02}\right)} \quad (3)$$

During the EC measurement period (25 June to 17 September 2015) the GPP was estimated as:

$$GPP = NEE_f - R_{eco} \quad (4)$$

Where NEE_f is the gap filled NEE according to Wutzler et al., (2018). This way R_{eco} and GPP become consistent with the measured and gap filled NEE. For the time before and after this period NEE was estimated as the sum of modelled R_{eco} and modelled GPP. The data for the GPP model was derived from:

$$GPP_m = NEE_m - R_{eco} \quad (5)$$

Where NEE_m is the measured net ecosystem exchange. The GPP_m was then fitted to a light response function:

$$GPP_m = c1 + c2 \cdot c3/(c2 + R_g) \quad (6)$$

4 Results

For CO_2 exchanges and partitioning we combined the soil efflux measurements with the chamber system with the eddy covariance flux measurements. This was crucial for the partitioning and for gap filling because from 20 April to 20 August at this location the sun is above the horizon 24 hours of the day and this means that there were few occasions of dark nighttime measurements with the eddy covariance system and all of these were collected at the very end of the summer. We consider the chamber measurements that were distributed across the summer to be more representative of R_{eco} for this location.

For CH_4 exchanges we don't have any eddy covariance measurements so we present only chamber data for this variable.

4.1Weather

The mean annual temperature at Kapp Linne was -1.5 ºC during 2015 which was 3.5ºC higher than the long-term mean (1961-1990) of -5.1 ºC. The summer (June-August) mean of 5.5 ºC was

2.0 ºC higher than the long-term mean for the same time period (Fig. 1). The summer precipitation in 2015 was much lower, 58 mm as compared to the long-term precipitation which was 121 mm. The annual precipitation was also lower, 431 mm compared to the long-term precipitation which was 514 mm.

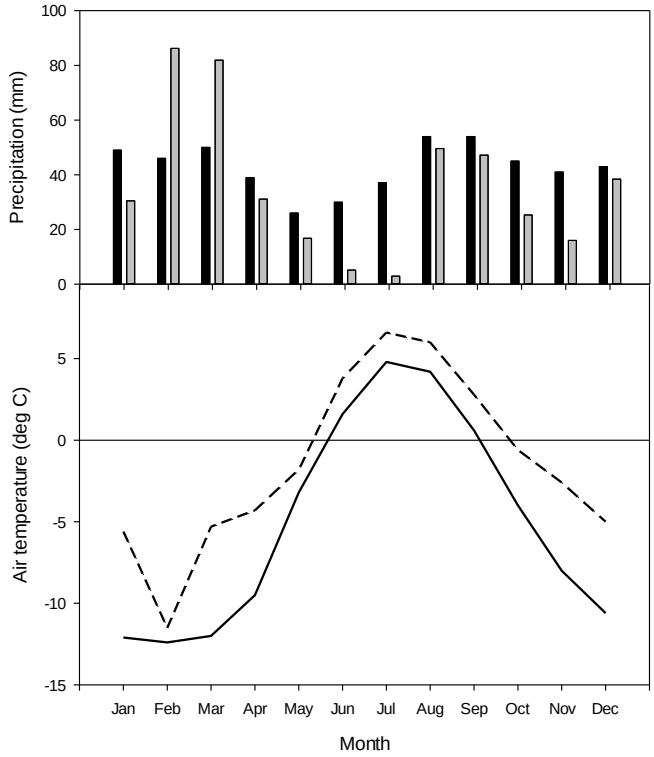

Figure 1. Monthly precipitation (top): Long-term average 1961-1990 black bars and 2015 grey bars. Data from Barentsburg for January-May, from Isfjord Radio for June-December. Mean monthly air temperature (bottom): Solid line is long-term average 1961-1990 and dotted line is 2015. Data from Isfjord Radio which is located about 1 km west of the investigation area.

We defined the start of the growing season (the period during which vegetation is photosynthesizing) in two different ways. The first (denoted Season 1, day no. 140; see Fig. 2) based on when daily air temperature started to stay above zero more steadily and the second (denoted Season 2, day no. 160) when most of the snow had disappeared. The ending of the growing season was defined as when the air temperature fell more steadily below zero, when ground ice began to establish and when a significant snow pack was established (day no. 284; Fig. 2).

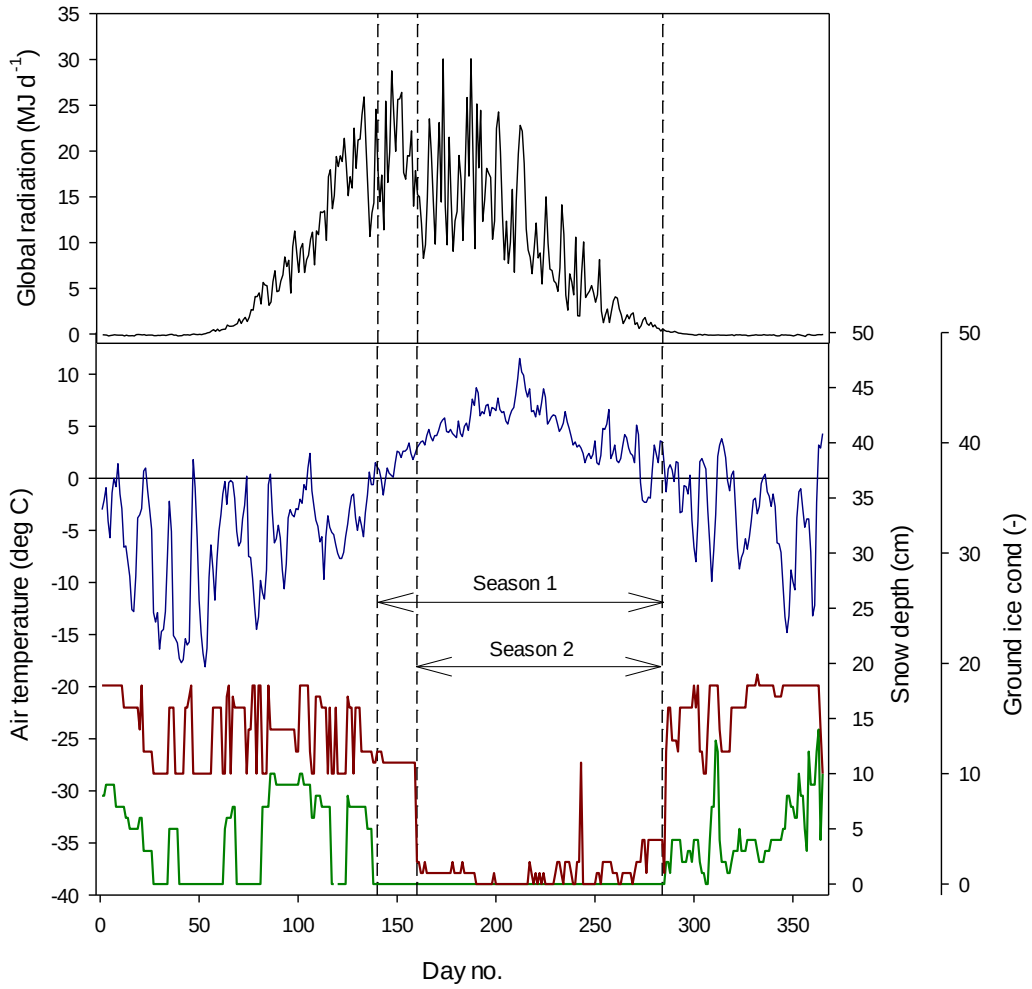

Fig. 2 Weather conditions during 2015. Top panel: Mean daily global radiation at Adventdalen. Bottom panel: Mean daily air temperature at Isfjord Radio (blue), snow depth (red) and ground ice conditions (green) at Svalbard airport close to Longyearbyen. The ground ice condition is scaled from 0 to 20 where 0 is no snow or ice on the ground and 20 indicate a complete cover of snow or ice.

4.2 Flux footprint and greenness

The footprint climatology shows a good representativity of the moss tundra surface by the EC measurements with 60-70% of fluxes emanating from areas well within the border of the tundra (Fig. 3). The mean green index for a circular area with radius of 100 m centered at the flux tower was 0.34 which corresponded exactly to the mean value for all chamber locations. The GI for the 24 chamber locations varied between 0.316 and 0.369. We observed a good (visual) correlation between GI and coverage of green plants (see Figures S4a-S4y of chamber location pictures and GI).

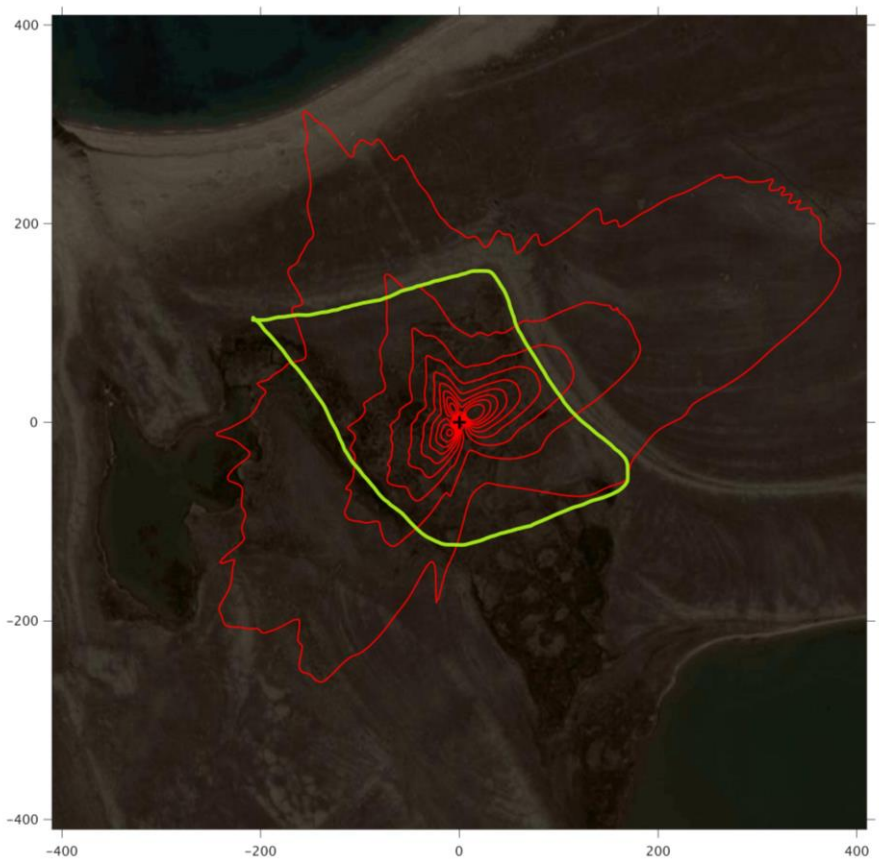

Figure 3. The footprint climatology with red contour lines 10-90%. The area within the green line mark the heart of the moss tundra. The scale (m) is shown on the outer borders of the picture.

4.3 CO_2 exchanges

The CO_2 fluxes from the chamber measurements showed quite large variation over time (Fig. 4) and across sampling locations (Fig. 5). The mean CO_2 flux of all samples was 0.81±0.11 µmol $m^{-2}s^{-1}$. The uncertainty is given as the 95 confidence limit.

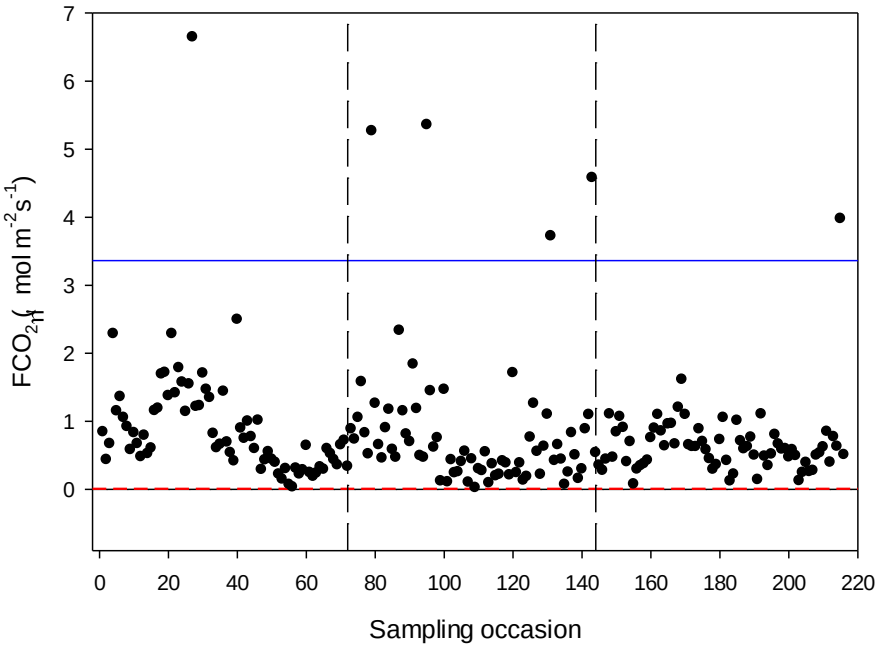

Figure 4. Measured CO_2 exchange from the 24 sampling points using dark chamber and portable gas analyzer. The dashed red line indicates CO_2 flux detection limit and the blue line represents 3xS.D. of all data points. The dashed vertical lines separate sampling periods from left to right: early summer, mid-summer and late-summer.

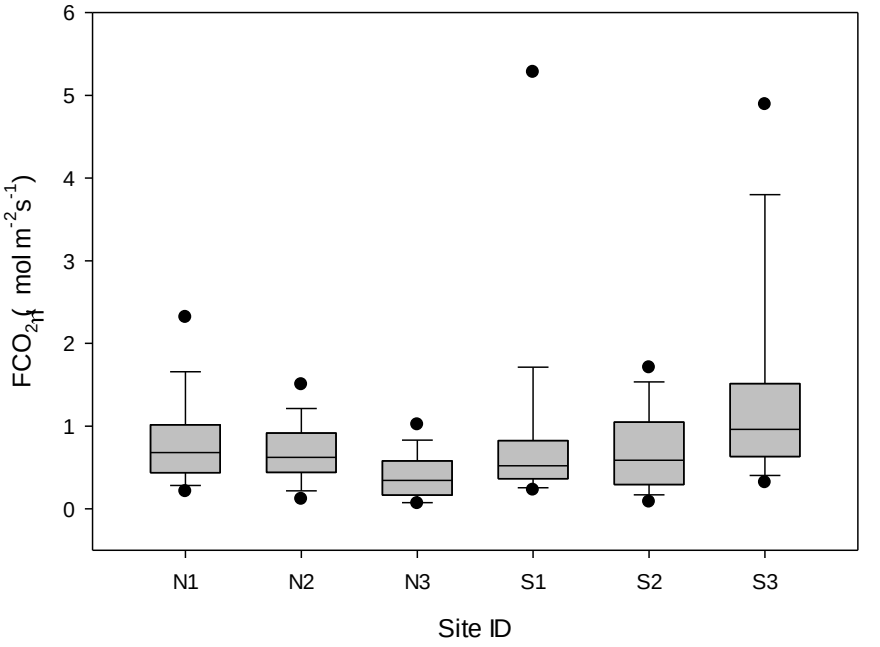

Figure 5. Box plot of CO_2 fluxes per sampling location named N1-N3, S1-S3. The boundaries of the grey boxes represent the 25% and 75% percentiles, the line represent the median, whiskers above and below the boxes indicate the 10% and 90% percentiles. Outlaying points are also shown.

Of the tested environmental variables T_a, θ, T_s, ALD, S_{id} and GI it was only T_a, θ and GI that contributed positively and significantly in decreasing order to explain the variability of the CO_2 flux (Table 1).

Table 1. Result of stepwise linear regression with CO_2 flux as dependent variable. Normality test failed but significance in all variables was confirmed with Wilcoxon Signed rank tests.

Variable	Partial-R^2	Probability (p)
T_a	0.190	<0.001
θ	0.037	0.002
GI	0.023	0.002

Ideally all of these variables should be used in a model to estimate R_{eco} for gap filling purposes but we could only use air temperature since this was the only variable that we had access to with complete coverage for a full year. The Lloyd &Taylor model (Eq. 3 & Fig. 6)) was thus used to estimate ecosystem respiration for 2015 using half-hourly air temperature as input.

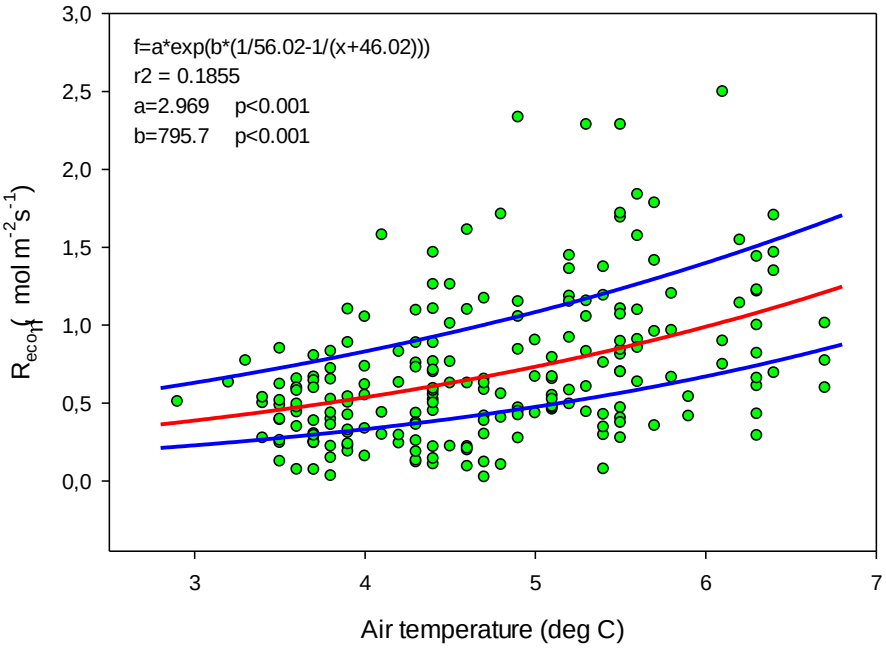

Figure 6. Measured ecosystem respiration (green dots) plotted against air temperature. The red curve is the fitted equation and the blue curves are the corresponding boundaries when considering the standard deviation of the parameters.

The modelled gross primary productivity (Eq. 6; GPP_m) had a small offset when global radiation was zero (Fig. 7). This offset was adjusted for when the model was applied for gapfilling so that GPP become zero during nighttime.

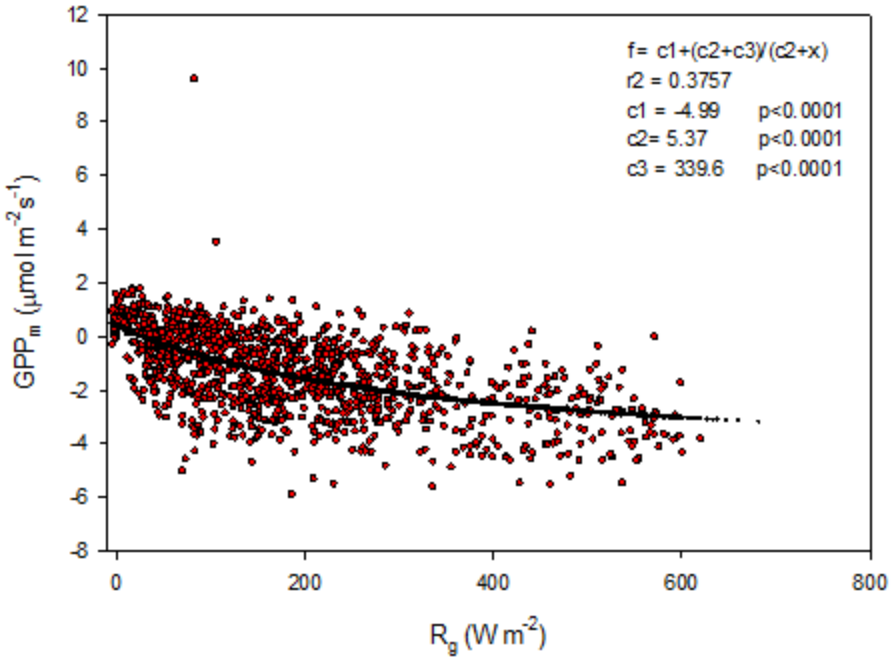

Figure 7. GPP_m plotted against global radiation; red symbols are estimated values according to eq. (5) and the black symbols are the fitted model.

We assumed that GPP was zero for the periods outside of the growing season and that our R_{eco} model was valid during winter as well as during growing season. The mean bi-weekly fluxes show that NEE is negative from about one week into June until one week into August (Fig. 8). The mean NEE is relatively constant during this period with a low -0.5 µmol $m^{-2}s^{-1}$. The maximum bi-weekly GPP is about -2.5 µmol $m^{-2}s^{-1}$ while the corresponding R_{eco} is about 2.0 µmol $m^{-2}s^{-1}$. The GPP become positive during one period in the autumn indicating an underestimation of R_{eco} during that time.

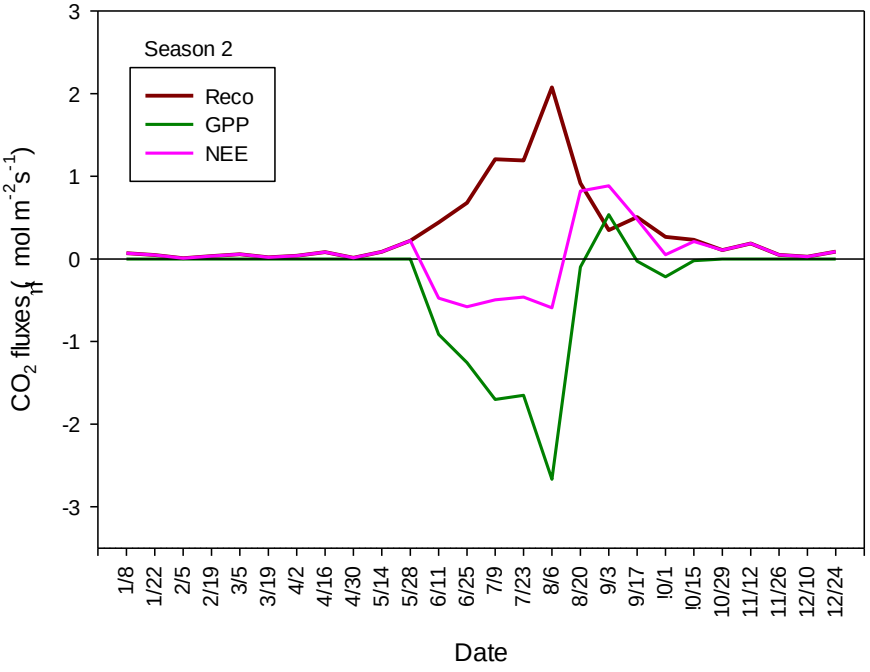

Figure 8. Bi-weekly gap filled CO_2 fluxes for season 2 (see Fig. 2) at Tunsjömyren, Kapp Linne during 2015.

The annual modelled and gap filled NEE was negative, -25.3 gC m^{-2} for season 1 and positive, 15.2 gC m^{-2} for season 2. The gapfilled NEE (Table 2) during the summer (June-August) was -37 g C m^{-2} or -0.40 g C m^{-2} day^{-1} which is good agreement with the measured NEE (25 June -31 August) with a mean daily uptake of -0.40 g C m^{-2} day^{-1}. A summary of all components for the different seasons are presented in Table 2.

Table 2. Summary of annual and seasonal C-fluxes from Kapp Linne.

Period	Component (gC m^{-2})	Season	
		1	2
Winter	Reco	15.8	21.2
	GPP	0	0
	NEE	15.8	21.2
Growing season	Reco	114.9	109.5
	GPP	-156.8	-116.3
	NEE	-41.9	-6.8
Summer (June-August)	Reco	97.8	97.8
	GPP	-134.8	-134.8
	NEE	-37.0	-37.0
Annual	Reco	131.5	131.5
	GPP	-156.8	-116.3
	NEE	-25.3	15.2

4.4 Temperature sensitivity of R_{eco} and GPP

The temperature sensitivity of the R_{eco} is already given by the fitted Lloyd & Taylor (1994) equation. In the absence of long time series of measurements during multiple year were natural climate variability could be used to assess temperature sensitivity of GPP we approached this problem in the following way. We normalize GPP for its dependence on radiation by estimating the difference between the 'measured' GPP and the model which only depends on radiation (see Fig. 7). The resulting normalized GPP show a dependence on air temperature (Fig. 9) with values becoming more negative with increasing temperature. We fitted the same type of model to these data as for the R_{eco} to be able to compare sensitivities to temperature.

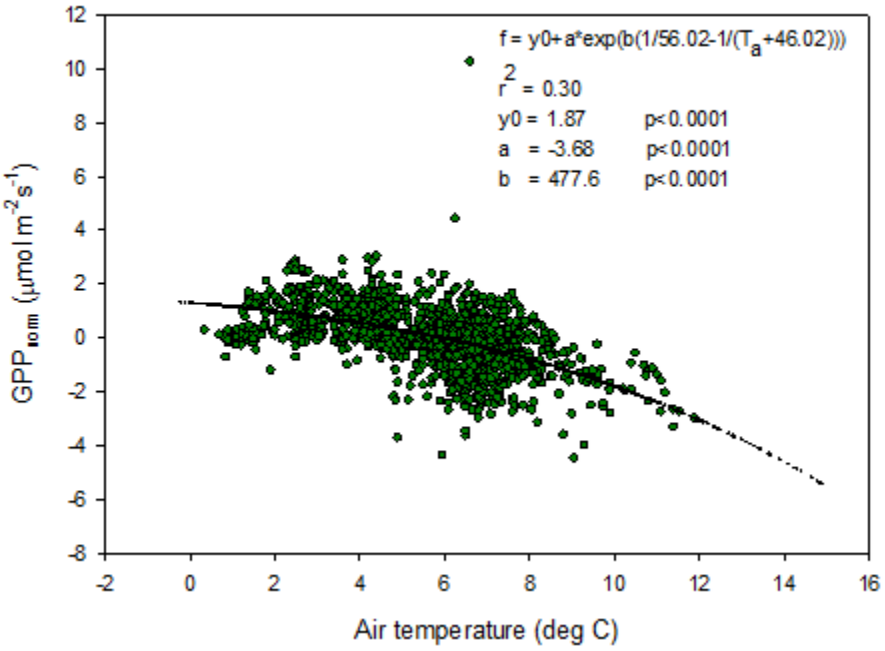

Figure 9. Normalized GPP plotted against air temperature and with the fitted exponential model.

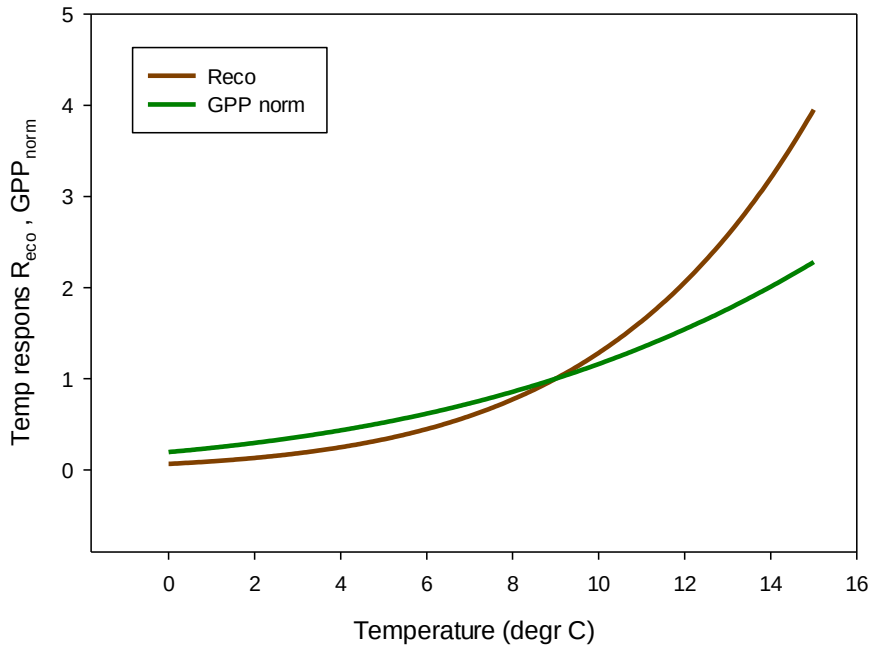

Figure 10. Temperature sensitivity for R_{eco} (brown) and R_g-normalized (positive) GPP (green).

In Fig. 10 we reversed the sign of the GPP temperature response function to make it more easily comparable with the R_{eco} response model. The temperature sensitivity (µmol $m^{-2}s^{-1}$ K^{-1}) can be estimated from the slope of these curves and the sensitivity is slightly higher for GPP than for R_{eco} in the interval 0 – 4.5 ºC, thereafter the difference is small up to about 7 ºC then it began to raise rapidly for R_{eco}. We tested what impact this could have by increasing the measured half-hourly air temperature by 1 ºC and found that during the growing season (season 2) the GPP increased by -3.89 gC m^{-2} and R_{eco} by 3.53 gC m^{-2}. Thus, a minor increase of GPP compared to R_{eco}. However, a one-degree higher winter temperature resulted in an addition respiration of 9 gC m^{-2}. Thus, an estimated loss of 8.5 gC m^{-2} for the whole year.

4.5 CH_4 exchanges

The CH_4 fluxes from the chamber measurements showed large variation over time (Fig. 10) and across sampling locations (Fig. 11). The mean CH_4 flux of all samples was 0.00051±0.00024 µmol $m^{-2}s^{-1}$. The uncertainty is given as the 95% confidence limit. Setting all fluxes that fell within the flux detection limits to zero changed the mean value with -0.2%. Assuming that the mean flux was representative for the whole of growing season 1, the total CH_4 summer emission was 0.039 to 0.164 g CH_4 m^{-2}. Converting this to CO_2 equivalents (CO_2-eq; GWP=34) we get a range of 1.3 to 5.6 g CO_2-eq for the summer and if we add also a possible winter emission of 22% of the annual (following Bao et al. 2021) we obtain an annual mean of 4.2±2.6 g CO_2-eq.

We also noticed a clear trend during the summer with highest fluxes in mid-June and then decreasing during the following two sampling occasions. The respective mean values with 95% confidence intervals for the three sampling periods were 0.00121±0.000512 µmol $m^{-2}s^{-1}$(June 14-

15), 0.000332±0.000465 µmol $m^{-2}s^{-1}$(June 26- July 2) and -0.00000781±0.0000936 µmol $m^{-2}s^{-1}$(August 25-26).

For CH_4 exchanges we found *ALD,* θ and *GI* to contribute significantly to explain the variance of the flux (Table 3). The CH_4 flux responded negatively to increasing ALD and positively to θ and *GI*.

Table 3. Result of stepwise multiple linear regression with CH_4 flux as dependent variable. Normality test failed but significance in all variables was confirmed with Wilcoxon Signed rank tests.

Variable	Delta-R^2	Probability (p)
ALD	0.175	<0.001
θ	0.025	0.01
GI	0.020	0.004

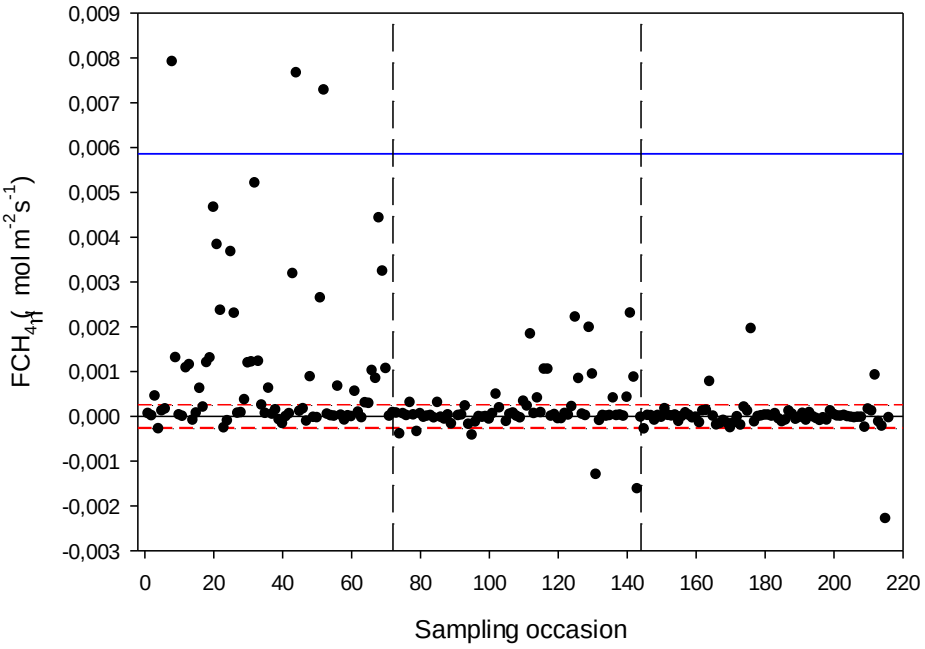

Figure 11. Measured CH_4 exchange from the 24 sampling points using dark chamber and portable gas analyzer. The dashed red lines indicate CH_4 flux detection limit, (i.e. inside the limits of detection the exact numbers are highly uncertain) and the blue line represents 3xS.D. The dashed vertical lines – same as in Fig. 4.

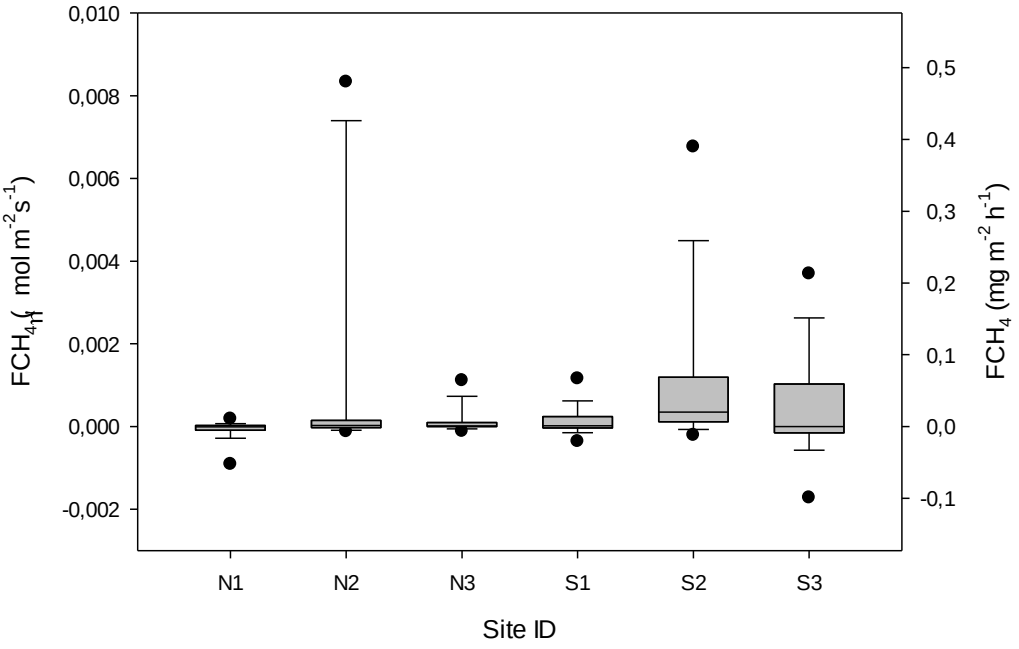

Figure 11. Box plot of CH_4 fluxes per sampling location named N1-N3, S1-S3. The statistics includes also the data that fall within the flux detection limits. The boundaries of the grey boxes represent the 25% and 75% percentiles, the line represent the median, whiskers above and below the boxes indicate the 10% and 90% percentiles. Outlaying points are also shown.

5 Discussion

5.1 Annual and seasonal CO_2 fluxes

We focus our discussion mainly on comparison with other tundra sites located in the North Atlantic area since these sites are influenced by the North Atlantic Current with its impact on weather patterns and climate. This limits the comparisons to sites in Greenland, Svalbard and Northern Scandinavia. However, we broaden the comparison a bit by adding two sites from Alaska.

Our annual NEE was in the range -25.3 to 15.2 gC m^{-2} depending on definition of growing season (Table 2). We judge the latter value to be more realistic since season 1 includes an unrealistically high GPP when there is still a snow cover on the ground in early spring. Lund et al. (2012) found that the start of the uptake period was strongly correlated with start of the snowmelt for the fen in Zackenberg, NE Greenland. They defined the start of snowmelt as the day when snow depth was <0.1 m. This coincides very well with our definition of start of growing season 2 (see Fig. 2). Soegaard and Nordtroem (1999) reported an annual NEE of -64.4 gC m^{-2} for the fen in Zackenberg and Pirk et al. (2017) reported -82 gC m^{-2} for an alluvial fen in Adventdalen, Svalbard, not far from Kapp Linne. For a site on the west coast of Greenland, Disco island with heath vegetation, Zhang et al. (2019) reported an annual NEE of -25±15 gC m^{-2}. Christensen et al. (2012) reported a range of -20 to -95 gC m^{-2} for annual NEE in a palsa mire in Abisko, Northern Sweden. Our results are closer to the values found for a sparsely vegetated

catchment area in Bayelva, Ny-Ålesund were Lüers et al. (2014) reported annual NEE to be 0 gC m^{-2}. If we go beyond the North Atlantic area to the low Arctic region in North America we can find sites that has a positive NEE on annual basis, 13.6 gC m^{-2} for a tussock tundra near Atquasuk, Alaska (Oechel et al., 2013) and 21-61 gC m^{-2} for a heath and 2-82 gC m^{-2} for a wet sedge ecosystem in Imnavait creek (Eurkirchen et al., 2012).

Lund et al. (2012) analysed 10 years of EC flux measurements from a heathland in Zackenberg and they reported a NEE range of -39.7 to -4.3 gC m^{-2} for the growing season. Our result for the growing season NEE of -6.8 gC m^{-2} (Season 2; Table 2) fall within the same range but it was only two years out of ten that showed that low uptake in Zackenberg heath. Their measured growing season GPP was in the range of -95.4 to -54.1 gC m^{-2} and the R_{eco} was in the range of 37.7 to 63.8 gC m^{-2}. Our corresponding values were -116.3 gC m^{-2} for GPP and 109.5 gC m^{-2} for R_{eco}. López-Blanco et al. (2017) presented data over a period of eight years of EC flux measurements from Kobbefjord, SW Greenland over an area of mixed fen and heath vegetation. Their growing season ranges were; for NEE -74.2 to -45.9 gC m^{-2}, for GPP -316.2 to – 181.8 gC m^{-2} and for R_{eco} it was 144.2 to 279.2 gC m^{-2} excluding 2011 which was anomalous because of a pest outbreak and 2014 which did not have a full growing season.

Our EC measurements of summer (June-August) NEE of -37 gC m^{-2} (Table 2) is in-between ranges reported for fen type of vegetation in NE Greenland; -96.3 gC m^{-2} (Soegaard and Nordstroem 1999) to -50 gC m^{-2} (Rennermalm et al. 2005) and heath vegetation; -1.4 to -18.9 gC m^{-2} (Groendahl et al. 2007).

It is difficult to compare growing season values because they are rarely defined the same way. Only small differences in definition of start and end of growing season can have a large impact on the NEE values since NEE is the sum of two large components of almost equal size and of different sign. In our case a 20 days difference in the beginning of the season changes growing season NEE from -25.3 to 15.2 gC m^{-2}. It is also difficult to compare GPP and R_{eco} for any season since the methods to split NEE into components differ from case to case. The most reliable comparison is probably for summer season (June – August) since most studies represents this period best in terms of measurement coverage and quality. So, with this in mind we are pretty confident with placing the C-exchange rates of the moss tundra intermediate between fen and heath type of vegetation in the North Atlantic region.

5.2 CH_4 fluxes

Our estimated growing season CH_4 flux of 0.08 gC m^{-2} is very low compared to most other methane emitting tundra sites; the Zackenberg fen site emitted CH_4 in the range 1.4 to 4.9 gC m^{-2} (Mastepanov et al. (2013), Jackowicz-Korczynski et al. (2010) reported 20.1 to 25.1 gCH_4 m^{-2} for the Stordalen mire in Northern Sweden. For three different sites in northern Alaska, Bao et al. (2021) reported annual emissions between 1.8 and 8.5 gCH_4 m^{-2} which corresponds to 0.94 and 4.5 gCH_4 m^{-2} for the growing season based on their estimate that growing season emissions are 52.6% of the annual emissions. Sachs et al. (2008) measured CH_4 exchanges with EC method in a northern Siberian polygon tundra and found generally low fluxes of about 18.5 mgCH_4 m^{-2} day^{-1} with little variation over the growing season. This rate adds up to 2.3 g CH_4 m^{-2} for their four months long growing season.

It should be pointed out that we did not perform measurements during the shoulder seasons meaning that we probably underestimate the seasonal total. Importance of shoulder seasons was first pointed out by Mastepanov et al. (2008) which discovered a large burst of CH_4 at and after the onset of soil freezing. One interesting observation is that the main part of our CH_4 flux occurred during the sampling period 14-15 June 2016 which is about 30 days after snow melt. This is the time of the season when CH_4 emissions normally are peaking (Mastepanov et al. 2013). After that, the rates dropped to practically zero in late August (see Fig. 10).

If we sum up the annual net CO_2 and CH_4 fluxes expressed as CO_2-eq we find that the moss tundra is emitting in total 60 gCO_2-eq of which the methane stands for 7%. So even if the CH_4 fluxes are small, it still represents a significant global warming impact in relative terms.

The comparison between the different sites are hampered by the fact that they in most cases belong to different bioclimatic subzones with differences in climate and vegetation (Walker et al., 2005). The only site besides Kapp Linne that belong to subzone B is the one in Ny Ålesund. The other high Arctic sites Adventdalen and Zackenberg both belong to subzone C, the intermediate high/low Arctic sites Kobbefjord and Disco Island belongs to subzone D respectively C/D. The low Arctic site Atqasuk belong to subzone D and the Imnavait Creek belong to subzone E. The sub-Arctic Abisko is not classified by Walker et al. (2005) but based mean July air temperature it should belong to subzone E. These differences in climate and vegetation should be kept in mind when comparing results from different sites.

5.3 Environmental controls of fluxes

A key issue in high Arctic is how ecosystems with soil that contain large amounts of frozen carbon will respond to warming. A recent report about the future climate of Svalbard (Hanssen-Bauer et al. 2019) show that appalling changes are at risk to occur. By 2071-2100 compared to 1971-2000 the mean annual temperature is estimated to increase by 7 ºC to 10 ºC for the medium and high emission scenarios, respectively. Precipitation is also estimated to increase by 45% respectively 65% for these scenarios. Such large changes will of course also have a lot of other impacts as well for instance shorter snow season, more erosion and sediment transport, changes in vegetation composition and growth etc etc. Assessment of such large changes are very difficult and is far beyond the scope of this paper. We have however shown that for a smaller temperature increase of 1 degree, the impact on the net carbon balance during the growing season will be minute; the increase in ecosystem respiration is compensated for by a corresponding, or actually slightly larger increase of gross primary productivity. Similar compensation effect was obtained for a heath site in Zackenberg by Lund et al. (2012). They used multi-year measurements to assess the effect of changes in temperature on the growing season fluxes. But, if we also consider an increase in temperature during winter, it is most likely that the annual NEE becomes weakened. It is not unlikely that the impact of climate change with higher temperature that is already a reality in Svalbard can be the reason why the annual NEE now is positive, i.e. the moss tundra is a GHG source of CO_2 to the atmosphere.

We found that air temperature was the main control of ecosystem respiration followed by soil moisture and greenness index (Table 1). We had expected that soil temperature should contribute

significantly to explain the variations in R_{eco} but it did not. Cannone et al. (2019) showed that ground surface temperature at 2 cm depth contributed significantly to explain R_{eco} in nearby Adventdalen during early, peak and late parts of the growing season. In their study soil moisture was also significant during peak and late seasons. One possible explanation to this difference in responses could be that our soil temperature was measured at 5 cm depth and that air temperature was more representative for the microbial processes taking place in or near the soil surface. Interestingly, GI contributed significantly to explain variations in R_{eco}. The GI was clearly correlated with the abundance of Salix polaris (see Supplement) and thus we interpret the positive correlation between GI and R_{eco} to be an effect of increasing contribution by autotrophic respiration to the total respiration.

We found no significant correlation between CH_4 emission and temperature. The best explanation was by active layer depth followed by soil moisture and GI (Table 3). But it should be pointed out that ALD and θ are not independent from each other and that ALD can be regarded as a proxy for any seasonal variability, like plant phenology. Soil moisture decreases with increasing active layer depth. The correlation between GI and CH_4 emission is probably also connected with abundance of Salix polaris which is a vascular plant. Vascular plants are since long mentioned as a pathway for CH_4 from the soil interior to the atmosphere in wet tundra ecosystems (e.g. Schimel 1995) but it could also be an effect of mediation of soil by the root exudation of organic acids as mentioned by Ström et al. (2012). However, we have not found any studies supporting the latter hypothesis concerning Salix polaris.

6 Conclusions

Our analyses of EC and chamber flux measurements have shown that the moss tunda on Kapp Linne is a small source of CO_2 and an even smaller source of CH_4 on an annual basis. Concerning the magnitude of the CO_2 exchanges during summer we find it to be in between those of fens and heath ecosystems located in the North Atlantic region. The CH_4 exchange is much lower than for other tundra ecosystems in the region.

The temperature sensitivity for CO_2 exchange was slightly higher for GPP than for R_{eco} in the low temperature range of 0-4.5 ºC, almost similar up to 7 ºC and thereafter it was considerably higher for R_{eco}. The consequence of this, for a small increase in air temperature of 1 degree (all other variables assumed unchanged) was that the increases in the two fluxes practically evened out during the growing season. But a warmer winter period would probably result in an increased loss of carbon. We cannot rule out that the reason why the moss tundra is a net source today is an effect of the warming that has already taken place in Svalbard.

606 The analysis of which environmental factors that controlled the small-scale fluxes showed that
607 air temperature dominated for R_{eco} and active layer depth for CH_4 but we also found that
608 greenness index significantly explained part of the variation in these fluxes. For R_{eco} we
609 attributed this to an increased share of autotrophic respiration to the total and for CH_4 we
610 hypothesized that the abundance of the woody shrub *Salix polaris* effected the exchange either
611 through internal plant pathway for methane or through increased provision of C substrate to the
612 anaerobic microbial community stimulating the production of methane. This finding is an
613 indication that modeling of CO_2 as well as of CH_4 fluxes can be improved by also considering
614 differences and changes in greenness of the vegetation.

615 **Acknowledgments, Samples, and Data**

616 This work did not receive any other funding except salaries for the authors from their respective
617 organizations. Observations of air temperature, relative humidity, precipitation, ground ice
618 conditions and snow depth were obtained from Norwegian Centre for Climate Services (NCCS)
619 and provided under licence CC BY 4.0. Global radiation data from Adventdalen was obtained
620 from the University Centre in Svalbard (UNIS). Thanks to associated professor Jonas Åkerman,
621 Lund University for support with information about the site. Data can be obtained from
622 https://zenodo.org.
623

624 **References**

625 Bao, T., Xu, X., Jia, G., Billesbach, D.P. & Sullivan, R.C. (2021). Much stronger tundra methane
626 emissions during autumn freeze than spring thaw. *Global Change Biology*, 27, 376–387.
627 https://doi.org/ 10.1111/gcb.15421

628 Bosiö, J., Stiegler, C., Johansson, M., Mbufong, H. N. & Christensen, T. R. (2014). Increased
629 photosynthesis compensates for shorter growing season in subarctic tundra—8 years of
630 snow accumulation manipulations. *Climatic Change*, 127, 321–334.
631 http://doi.org/10.1007/s10584-014-1247-4

632 Burba, G. G., McDermitt, D., Grelle, A., Anderson, D.J. & Xu, L. (2008). Addressing the
633 influence of instrument surface heat exchange on the measurements of CO_2 flux from
634 open-path gas analyzers. *Global Change Biology*, 14, 1854–1876.
635 https://doi.org/10.1111/j.1365-2486.2008.01606.x

636 Callaghan, T.V., Björn, L O., Chapin III, F.S., Chernov, Y., Christensen, T.R., Huntley, B., Ims,
637 R., Johansson, M., Jolly Riedlinger, D., Jonasson, S., Matveyeva, N., Oechel, W.,
638 Panikov, N. & Shaver, G. (2005). Arctic tundra and polar desert ecosystems. In: ACIA
639 (Ed.), *Arctic Climate Impact Assessment*, (pp. 243-352). Cambridge University Press.

640 Cannonea, N., Pontib, S., Christiansen, H.H., Christensen, T.R., Pirk, N. & Guglielmin, M.
641 (2019). Effects of active layer seasonal dynamics and plant phenology on CO_2 land
642 atmosphere fluxes at polygonal tundra in the High Arctic, Svalbard. *Catena*, 174, 142-
643 153. https://doi.org/ 10.1016/j.catena.2018.11.013

644 Christensen, T.R., Johansson, T., Akerman, H.J. & Mastepanov, M. (2004). Thawing sub-arctic
645 permafrost: Effects on vegetation and methane emissions. *Geophysical Research Letters*,
646 31, L04501. https://doi.org/10.1029/2003GL018680

647 Christensen, T.R., Jackowicz-Korzynski, M., Aurela, M., Crill, P., Heliasz, M., Mastepanov, M.
648 & Friborg, T. (2012). Monitoring the Multi-Year Carbon Balance of a Subarctic Palsa
649 Mire with Micrometeorological Techniques. *Ambio*, 41, 207–217.
650 https://doi.org/10.1007/s13280-012-0302-5

651 Euskirchen, E. S., Bret-Harte, M. S., Scott, G. J., Edgar, C., & Shaver, G. R. (2012). Seasonal
652 patterns of carbon dioxide and water fluxes in three representative tundra ecosystems in
653 northern Alaska, *Ecosphere*, 3, 1–19. https://doi.org/10.1890/ES11-00202.1
654 Euskirchen, E.S., Bret-Harte, M.S., Shaver, G.R., Edgar, C.W., & Romanovsky, V.E. (2017).
655 Long-Term Release of Carbon Dioxide from Arctic Tundra Ecosystems in Alaska.
656 *Ecosystems*, 20, 960–974. http://doi.org/10.1007/s10021-016-0085-9

657 Friedlingstein, P., Cox, P., Betts, R., Bopp, L., von Bloh, W., Brovkin, V., Cadule, P., Doney, S.,
658 Eby, M., Fung, I., Bala, G., John, J., Jones, C., Joos, F., Kato, T., Kawamiya, M., Knorr,
659 W., Lindsay, K., Matthews, H. D., Raddatz, T., Rayner, P., Reick, C., Roeckner, E.,
660 Schnitzler, K. G., Schnur, R., Strassmann, K., Weaver, A. J., Yoshikawa, C., & Zeng, N.
661 (2006). Climate-carbon cycle feedback analysis: Results from the C4MIP model
662 intercomparison, *J. Climate*, 19, 3337–3353. https://doi.org/10.1175/JCLI3800.1

663 Friedlingstein, P., O'Sullivan, M., Jones, M.W. et al. (2019). Global carbon budget 2010. *Earth*
664 *Syst. Sci. Data*, 12, 3269–3340. https://doi.org/10.5194/essd-12-3269-2020

665 Groendahl, L., Friborg, T., & Soegaard, H. (2007). Temperature and snow-melt controls on
666 interannual variability in carbon exchange in the high Arctic. *Theor. Appl. Climatol.*, 88,
667 111–125. http://doi.org/10.1007/s00704-005-0228-y

668 Hanssen-Bauer, I., Førland, E.J., Hisdal, H., Mayer, S., Sandø, A.B. & Sorteberg, A. (2019).
669 Climate in Svalbard 2100 – a knowledge base for climate adaptation. *Report no. 1/2019.*
670 Norwegian Environment Agency.

671 Hugelius, G., Strauss, J., Zubrzycki, S., Haren, J.W., Schuur, E.A.G., Ping, C.-L., Schirrmeister,
672 L., Grosse, G., Michaelson, G.J., Koven, C.D., O'Donnell, J.A., Elberling, B., Mishra,
673 U., Camill, P., Yu, Z., Palmtag, J. & Kuhry, P. (2014). Estimated stocks of circumpolar
674 permafrost carbon with quantified uncertainty ranges and identified data gaps.
675 *Biogeosciences*, 11, 6573–6593. http://doi.org/10.5194/bg-11-6573-2014

676 Jackowicz-Korczynski, M., Christensen, T. R., Backstrand, K., Crill, P., Friborg, T.,
677 Mastepanov, M., & Strom, L. (2010). Annual cycle of methane emission from a subarctic
678 peatland. *J. Geophys. Res.-Biogeo.*, 115, G02009. http://doi.org/10.1029/2008JG000913

679 Kljun, N., Calanca, P., Rotach, M.W., & Schmid, H.P. (2015). A simple two-dimensional
680 parameterisation for Flux Footprint Prediction (FFP). *Geosci. Model Dev*., 8, 3695-3713.
681 http://doi.or/10.5194/gmd-8-3695-2015

682 Li-Cor (2016). EddyPro® Software (Version 6.0) Li-Cor Inc., Lincoln, USA.

683 Lloyd, J., & Taylor, J.A. (1994). On the temperature dependence of soil respiration. *Functional*
684 *Ecology*, 8(3), 315-323.

685 Lopez-Blanco, E., Lund, M., Williams, M., Tamstorf, M.P., Westergaard-Nielsen, A., Exbrayat,
686 J.-F., Hansen, B.U., & Chrostensen, T.R. (2017). Exchange of CO2 in Arctic tundra:
687 impacts of meteorological variations and biological disturbance. *Biogeosciences*, 14,
688 4467–4483. https://doi.org/10.5194/bg-14-4467-2017

689 Lund, M., Falk, J. M., Friborg, T., Mbufong, H. N., Sigsgaard, C., Soegaard, H., & Tamstorf, M.
690 P. (2012). Trends in CO2 exchange in a high Arctic tundra heath, 2000–2010. *J.*
691 *Geophys. Res.- Biogeo*. https://doi.org/10.1029/2011JG001901

692 Lüers, J., Westermann, S., Piel, K., & Boike, J. (2014). Annual CO2 budget and seasonal CO2
693 exchange signals at a high Arctic permafrost site on Spitsbergen, Svalbard archipelago.
694 *Biogeosciences*, 11, 6307–6322. http://doi.0rg/10.5194/bg-11-6307

695 Mastepanov, M., Sigsgaard, C., Dlugokencky, E. J., Houweling, S., Strom L., Tamstorf, M. P., &
696 Christensen, T. R. (2008). Large tundra methane burst during onset of freezing. *Nature*,
697 456, 628–631. http://doi.org/10.1038/nature07464

698 Mastepanov, M., Sigsgaard, C., Tagesson, T., Ström, L., Tamstorf, M. P., Lund, M., &
699 Christensen, T. R. (2013). Revisiting factors controlling methane emissions from high-
700 Arctic tundra. *Biogeosciences*, 10, 5139–5158. https://doi.org/10.5194/bg-10- 5139-2013

701 McGuire, A. D., Christensen, T. R., Hayes, D., Heroult, A., Euskirchen, E., Kimball, J. S.,
702 Koven, C., Lafleur, P., Miller, P. A., Oechel, W., Peylin, P., Williams, M., & Yi, Y.
703 (2012). An assessment of the carbon balance of Arctic tundra: comparisons among
704 observations, process models, and atmospheric inversions. *Biogeosciences*, 9, 3185–
705 3204. https://doi.org/10.5194/bg-9-3185- 2012

706 Myers-Smith, I. H., Kerby, J. T., Phoenix, G. K., Bjerke, J. W., Epstein, H. E., Assman, J. J.,
707 John, C., Adreu-Hayles, L., Angers-Blondin, S., Beck, P. S. A., Berner, L. T., Bhatt, U.
708 S., Bjorkman, A. D., Blok, D., Bryn, A., Christiansen, C. T., Cornelissen, J. H. C.,
709 Cunliffe, A. M., Elmendorf, S. C., Forbes, B. C., Goetz, S. J., Hollister, R. D., de Jong,
710 R., Loranty, M. M., Marcias-Fauria, K., Maseyk, K., Normand, S., Olofsson, J., Parker,
711 T. C., Parmentier, F-J. W., Post, E., Schaepman-Strub, G., Stordal, F., Sullivan, P. F.,
712 Thomas, H. J. D., Tømmervik, H., Treharne, R., Tweedie, C. E., Walker, D. A.,
713 Wilmking, M. & Wipf, S. (2020). Complexity revealed in the greening of the Arctic. *Nat.*
714 *Clim. Chang*., 10, 106–117. https://doi.org/10.1038/s41558-019-0688

715 Oechel, W. C., C. A. Laskowski, G. Burba, B. Gioli, & Kalhori, A.A.M. (2014). Annual patterns
716 and budget of CO2 flux in an Arctic tussock tundra ecosystem. *J. Geophys. Res.*
717 *Biogeosci*., 119, 323–339. http://doi.org/10.1002/2013JG002431

718 Pirk, N., Sievers, J., Mertes, J., Parmentier, F.-J. W., Mastepanov, M., & Christensen, T. R.
719 (2017). Spatial variability of CO_2 uptake in polygonal tundra: assessing low-frequency
720 disturbances in eddy covariance flux estimates. *Biogeosciences*, 14, 3157–3169.
721 https://doi.org/10.5194/bg-14-3157-2017

722 Post, E., Forchhammar, M. C., Bret-Harte, M. S., Callaghan, T. V., Christensen, T. R., Elberling,
723 B., Fox, A. D., Gilg, O., Hik, D. S., Høye, T. T., Ims, R. A., Jeppesen, E., Klein, D. R.,
724 Madesn, J., McGuire, A. D., Rysgaard, S., Schindler, D. E., Stirling, I., Tamstorf, M. P.,
725 Tyler, N. J. C., van der Wal, R., Welker, J., Wookey, P. A., Schmidt, M. & Astrup, P.
726 (2009). Ecological dynamics across the arctic associated with recent climate change.
727 *Science*, 325, 1355–1358. http://doi.org/10.1126/science.117311

728 Ravolainen, V., Soininen, E. M., Jónsdóttir, I. S., Eischeid, I., Forchhammer, M., van der Wal,
729 R. & Pedersen, A. Ø. (2020). High Arctic ecosystem states: Conceptual models of
730 vegetation change to guide long-term monitoring and research. *Ambio* 49, 666–677.
731 https://doi.org/10.1007/s13280-019-01310-x

732 Rennermalm, A.K., Soegaard, H., & Nordstroem, C. (2005). Interannual Variability in Carbon
733 Dioxide Exchange from a High Arctic Fen Estimated by Measurements and Modeling.
734 *Arctic, Antarctic, and Alpine Research*, 37(4), 545-556. https://doi.org/10.1657/1523-
735 0430(2005)037[0545:IVICDE]2.0.CO;2

736 Richardson, A. D., Braswell, B. H., Hollinger, D. Y., Jenkins, J. P. & Ollinger, S. V. (2009).
737 Near-surface remote sensing of spatial and temporal variation in canopy phenology.
738 *Ecological Applications*, 19: 1417–1428. http://doi.org/10.1890/08-2022.1

739 Sachs, T., Wille, C., Boike, J., & Kutzbach, L. (2008). Environmental controls on ecosystem-
740 scale CH_4 emission from polygonal tundra in the Lena river delta, Siberia. *J. Geophys.*
741 *Res.-Biogeosci*., 113, G00A03. http://doi.org/10.1029/2007JG000505

742 Saunois, M., Stavert, A.R., Poulter, B et al. (2020). The global methane budget 2000-2017. *Earth*
743 *Syst. Sci. Data*, 12, 1561–1623. https://doi.org/10.5194/essd-12-1561

744 Schimel, J.P. (1995). Plant Transport and Methane Production as Controls on Methane Flux from
745 Arctic Wet Meadow Tundra. *Biogeochemistry*, 28 (3), 183-200.
746 https://doi.org/10.1007/BF02186458

747 Schuur, E. A. G., McGuire, A. D., Schadel, C., Grosse, G., Harden, J. W., Hayes, D. J.,
748 Hugelius, G., Koven, C. D., Kuhry, P., Lawrence, D. M., Natali, S. M., Olefeldt, D.,
749 Romanovsky, V. E., Schaefer, K., Turetsky, M. R., Treat, C. C., & Vonk, J. E. (2015).
750 Climate change and the permafrost carbon feedback. *Nature*, 520, 171–179,
751 https://doi.org/10.1038/nature14338

752 Soegaard, H. & Nordstroem, C. (1999). Carbon dioxide exchange in a high-arctic fen estimated
753 by eddy covariance measurements and modeling, *Glob. Change Biol*., 5, 547–562.
754 https://doi.org/10.1111/j.1365-2486.1999.00250.x
755 Strom, L., Tagesson, T., Mastepanov, M., and Christensen, T. R. (2012). Presence of
756 Eriophorum scheuchzeri enhances substrate availability and methane emission in an
757 Arctic wetland. *Soil Biol. Biochem.*, 45, 61–
758 70.http://doi.org/10.1016/j.soilbio.2011.09.005
759
760 Walker, D. A., Raynolds, M. K., Daniëls, F. J. A., Einarsson, E., Elvebakk, A., Gould, W. A.,
761 Katenin, A. E., Kholod, S. S., Markon, C. J., Melnikov, E. S., Moskalenko, N. G., Talbot,
762 S. S., Yurtsev, B. A. & the other members of the CAVM Team (2005). The Circumpolar
763 Arctic vegetation map. *Journal of Vegetation Science*, 16, 267-282.
764 https://doi.org/10.1111/j.1654-1103.2005.tb02365.x
765
766 Vanderpuye, A. W., Elvebakk, A. & Nilsen, L. (2002). Plant communities along environmental
767 gradients of high-arctic mires in Sassendalen, Svalbard. *J. Veg. Sci.*, 13, 875–884.
768 http://doi.org/ 10.1111/*j*.1654-1103.2002.tb02117.x
769

770 Wutzler, T., Lucas-Moffat, A., Migliavacca, M., Knauer, J., Sickel, K., Šigut, L., Menzer, O.,
771 Reichstein, M. (2018). Basic and extensible post-processing of eddy covariance flux data
772 with REddyProc. *Biogeosciences*, 15(16), 5015-5030. Doi:10.5194/bg-15-5015-2018.

773 Zhang, W., Jansson, P-E., Sigsgaard, C., McConnella, A., Jammet, M.M., Westergaard-Nielsen,
774 A., Lund, M., Friborg, T., Michelsen, A., & Elberling, B. (2019). Model-data fusion to
775 assess year-round CO2 fluxes for an arctic heath ecosystem in West Greenland (69°N).
776 *Agricultural and Forest Meteorology*, 272-273, 176-186.
777 https://doi.org/10.1016/j.agrformet.2019.02.021